Enzyme and Microbial Technology 57 (2014) 8–15

Contents lists available at ScienceDirect

Enzyme and Microbial Technology

journal homepage: www.elsevier.com/locate/emt

A novel horseradish peroxidase biosensor towards the detection of dopamine: A voltammetric study

P. Raghu, T. Madhusudana Reddy*, P. Gopal, K. Reddaiah, N.Y. Sreedhar

Electrochemical Research Laboratory, Department of Chemistry, S.V.U. College of Sciences, Sri Venkateswara University, Tirupati, 517502, Andhra Pradesh, India

ARTICLE INFO

Article history:
Received 25 July 2013
Received in revised form 2 January 2014
Accepted 4 January 2014
Available online 13 January 2014

Keywords:
Carbon paste electrode
Horseradish peroxidase
Glycine
Multiwalled carbon nanotubes
Silica sol–gel
Dopamine

ABSTRACT

A polymerized film of glycine (Gly) was prepared on the surface of carbon paste electrode (CPE) through the cyclic voltammetry (CV) technique. A novel biosensor for the determination of dopamine (DA) has been constructed based on horseradish peroxidase (HRP) and multiwalled carbon nanotubes (MWCNTs) immobilizing on Poly (Gly)/CPE through silica sol–gel (SiSG) entrapment. CV measurements were employed in order to understand the feasibility of poly (Gly) as an electron carrier between the immobilized peroxidase and the surface of CPE. By using differential pulse voltammetry (DPV) the calibration curves of DA was obtained in the range of 15–865 μM. The limit of detection (LOD) and limit of quantification (LOQ) of DA was found to be 6×10^{-7} M and 2×10^{-6} M respectively. The apparent Michaelis–Menten constant (K_m^{app}) was found to be 0.5 mM and illustrated that the good biological activity of the fixed enzyme. Electrochemical impedance spectroscopy (EIS) results confirmed the rapid electron transfer and also the immobilization of enzyme on the electrode surface. The biosensor showed high sensitivity, selectivity and reproducibility. This method has been used to determine DA in the presence of various interferences and in clinical preparations.

1. Introduction

Dopamine (DA) is one of the most typical catecholamine neurotransmitter, which mainly exists in mammalian brain tissues, fluids and plays a very important role in the central nervous system (CNS). When present in low concentration it is likely to give rise to neurodegenerative diseases such as Parkinson and Alzheimer [1]. DA is also widely applied in the treatment of circulatory collapse syndrome caused by myocardial infaraction trauma renal failure, cardiac surgery or congestic cardiac failure [2]. Numerous methods have been used for the detection of DA include chemiluminescence [3], flourimetry [4], ultraviolet spectroscopy [5], capillary electrophoresis [6], high performance liquid chromatography (HPLC) [7], ion chromatography [8] and electrochemical methods [9,10]. Among the above techniques the electrochemical techniques have gained more attention in many cases, due to fast in detections, low in cost and lower detection limits with good accuracy [9].

Carbon nanotubes (CNTs) are interesting materials for the fabrication of biosensing devices with enhanced sensitivity. The improvement of active surface area [11], their capability to facilitate redox reaction of many compounds [12], the increase in the sensitivity [13] advocate the use of nanotubes as key building blocks in fabricating the electrodes. Enzymatic electrochemical biosensing for medical purposes is one of the most promising applications of CNTs [14]. The CNTs have the capability to promote the electron transfer from enzyme to electrode surface. Actually, the multiwalled carbon nanotubes (MWCNTs) are mostly metallic and also reduce the fouling of enzymes [15]. Thus, MWCNTs is a better modifier for electrochemical applications [16].

Horseradish peroxidase (HRP) is one of the most widely studied enzymes in the development of enzyme based biosensors and this is due to easy availability and low cost. The enzyme contains heme as a prosthetic group, which is also the protein active site with the resting state of the heme–iron Fe (II); and it can catalyze the oxidation of a different substrates [17]. However, it is difficult for the immobilization of HRP on the electrode surface and hence it requires a specific immobilization method for immobilization of HRP. In the recent past several valuable immobilization strategies have been employed including absorption [18], cross linking [19,20], layer by layer assembly [21], sol–gel entrapment [22] and electro polymerization [23,24]. Among the above silica sol–gel technology has been utilized for the immobilization of a wide variety of biomolecules, due to its advantages, such as chemical inertness, physical rigidity, high thermal stability, biodegradation and optical transparency [25,26]. It has been widely used as an efficient fixing agent of biocatalyst on the electrode surface. Because of its good biocompatibility and film forming ability, the stability

* Corresponding author. Tel.: +91 877 2289303.
E-mail address: tmsreddysvu@gmail.com (T.M. Reddy).

0141-0229/$ – see front matter © 2014 Elsevier Inc. All rights reserved.
http://dx.doi.org/10.1016/j.enzmictec.2014.01.002

of the biosensors can be enhanced largely and also it has numerous biological sensing applications [27–30].

The present manuscript describes the immobilization of HRP and MWCNTs on a poly (Gly) modified carbon paste electrode. The electrocatalytic response to the oxidation of DA by using CV and DPV was studied. The modification process was characterized by CV. The factors influencing and the performance of the biosensor were studied in detail. The experimental results showed that the biosensor could be directly used for the determination of DA concentrations in clinical preparations with satisfactory results. The biosensor exhibited high sensitivity, selectivity, good repeatability and reproducibility.

2. Experimental

2.1. Reagents

All chemicals were obtained from commercial sources and used without further purification. Horseradish peroxidase (E.C. 1.11.1.7 type – VI-A – S/5 mg, Amoracia rusticana source, 1840 U/mg), Dopamine and glycine were purchased from Sigma–Aldrich chemicals Co. USA. Tetraethyl orthosilicate (TEOS), cetyltrimethyl ammonium bromide (CTAB), Triton X-100 were obtained from Sigma–Aldrich chemicals Co. USA. The graphite fine powder was procured from Loba Chemie Pvt. Ltd., Mumbai (INDIA) and silicon oil from Thermo Fisher Scientific India Pvt. Ltd., Mumbai (INDIA). Multiwalled carbon nanotubes (MWCNTs) were purchased from Dropsens, Edificio CEEI, Llanera (SPAIN). Phosphate buffer solution (PBS) was prepared by mixing 0.1 M disodium hydrogen phosphate and 0.1 M sodium dihydrogen orthophosphate. All the aqueous solutions were prepared with double distilled water. The enzyme stock solution and working solutions of chemicals were stored in refrigerator.

2.2. Apparatus

The electrochemical measurements were taken in a three electrodes cell at a room temperature of 25 ± 2 °C. The working electrode was an enzyme immobilized carbon paste electrode (HRP–MWCNTs–SiSG/Poly (Gly)/CPE). The reference electrode was a saturated calomel electrode system and glassy carbon rod electrode was used as an auxiliary electrode. Electrochemical measurements were carried out using CH – Electrochemical Analyzer (Model CHI – 660D, CH Instruments, USA). Elico U 120 pH meter combined with pH CL 51 B electrode was used for measuring the pH values.

2.3. Preparation of poly glycine modified carbon paste electrode (Poly (Gly)/CPE)

The carbon past electrode was prepared by hand mixing 85% graphite powder and 15% silicon oil in an agate mortar. The carbon paste was packed into the cavity of a homemade carbon paste electrode with a diameter of 2 mm and smoothed on a weighing paper [31,32]. The 0.01 M of glycine aqueous solution was placed in the electrochemical cell, the CPE was dipped and was scanned for four multiple cycles between the potential ranges from −0.5 V to +1.8 V at a scan rate of 100 mV s^{-1}. After the polymerization, the Poly (Gly)/CPE was rinsed sufficiently with double distilled water.

2.4. Fabrication of biosensor (HRP–MWCNTs–SiSG/Poly (Gly)/CPE)

A homogenous TEOS silica sol–gel was made by mixing 2 ml of TEOS, 1 ml of H_2O, 50 μl of 0.1 M HCl, 25 μl of 10% Triton X-100. The mixture was stirred for 1 h for obtaining clear sol. The sol can be stored for about 1 month when it was kept in refrigerator.

The 10 μl of 5 mg/ml HRP enzyme stock solution was added to the mixture of 10 μl of stock SiSG solution, 40 μl of 0.1 M PBS and 10 μl of 0.1 mg/ml MWCNTs. A drop of this dispersion with a volume of 5 μl was cast onto the surface of the Poly (Gly)/CPE, and then it was allowed to dry at room temperature for 3–5 min. The electrode was gently washed with PBS and was used for further experimental procedure [33]. The fabrication procedure of the biosensor was illustrated in Scheme 1.

3. Results and discussion

3.1. Electro polymerization of glycine at the surface of carbon paste electrode

Fig. 1 shows the electropolymerization of glycine on the surface of carbon paste electrode through CV. The positive potential in the potential scan range was the most important factor in preparing the polymer film, when the potential scan window was between

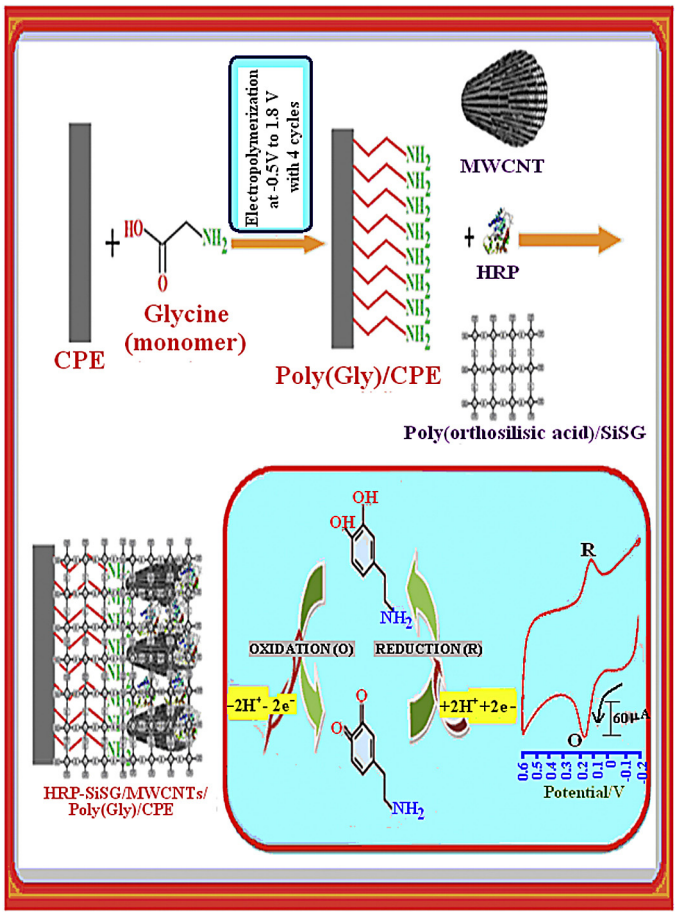

Scheme 1. A schematic diagram showing the various steps involved in the construction of HRP–MWCNTs–SiSG/Poly (Gly)/CPE and with working principle for the determination of DA.

−500 mV and +1200 mV, it was observed that there was no polymer formation on the electrode surface, but when extended from −500 mV to +1800 mV the effective polymerization was observed. When the potential window was extended in negative direction the polymerization was not observed. Hence the potential window between −500 mV and +1800 mV was considered for the effective polymerization process. The experimental results showed that in the first scan a broad voltammogram was obtained which goes on increasing with increase in the number of cycles indicating the

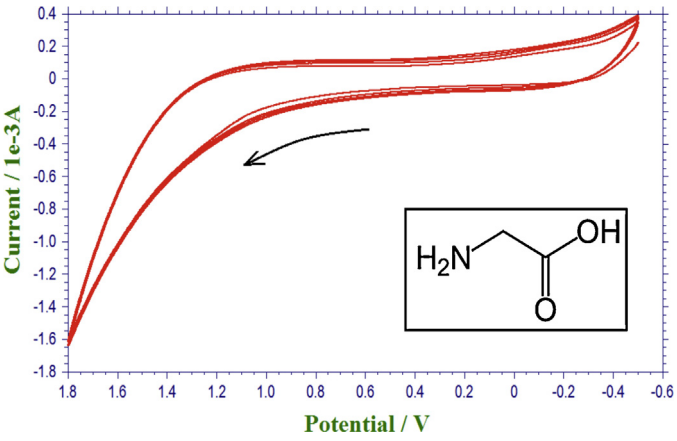

Fig. 1. Cyclic voltammogram for the electrochemical polymerization of glycine at the CPE.

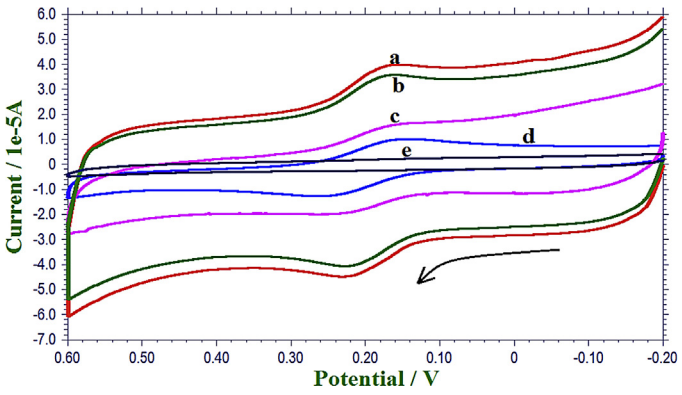

Fig. 2. Cyclic voltammmograms recorded at (a, e) HRP–MWCNTs–SiSG/Poly (Gly)/CPE, (b) HRP–SiSG/poly (Gly)/CPE, (c) HRP–SiSG/CPE, (d) CPE in 1 M KCl solution containing 1 mM $K_4[Fe(CN)_6]$, (e): in the buffer solution.

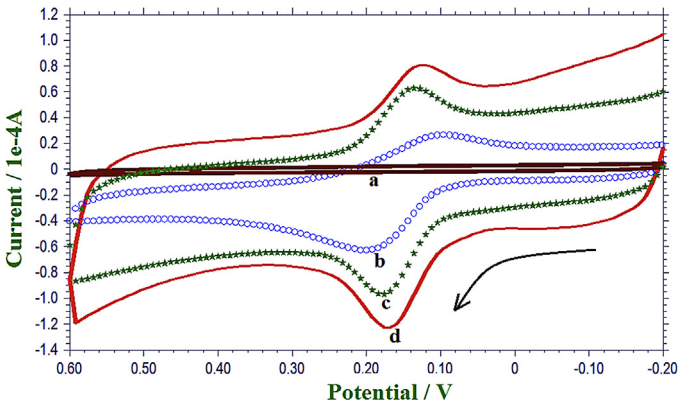

Fig. 3. Cyclic voltammograms of (a, d) HRP–MWCNTs–SiSG/Poly (Gly)/CPE, (b) CPE, (c) MWCNTs/poly (Gly)/CPE in 0.1 M PBS (pH 7.0)/1 M KCl (a) and 1 mM DA (b, c and d) at scan rate of 50 mV s^{-1}.

formation of electro conductive polymer film on the electrode surface. The fabricated polymer film electrode was then washed with distilled water to remove the physically adsorbed material and was used for further electrochemical analysis.

3.2. Electrochemical characterization of assembly process of HRP–MWCNTs–SiSG/Poly (Gly)/CPE

Fig. 2 shows the cyclic voltammograms for the different assembly stages of the biosensor in 1 mM K_4 [$Fe(CN_6)$] solution prepared by 0.1 M PBS (pH 7.0)/1 M KCl, where the curves (a and e) express HRP–MWCNTs–SiSG/Poly (Gly)/CPE, curve 'b' express HRP–SiSG/Poly (Gly)/CPE, curves 'c' and 'd' were HRP–SiSG/CPE and bare CPE respectively. From the curves 'c' (Ip_a = 8.6 μA and Ep_a = 0.265 V) and 'd' (Ip_a = 9.3 μA, Ep_a = 0.264 V, Ip_c = 8.9 μA and Ep_c = 0.142 V), it can be observed that the peak currents decrease significantly and also the cathodic peak shape was demolished after assembling HRP–SiSG on the bare CPE, this is due to the hindering of electron transfer by the enzyme. This also proved that the HRP–SiSG was assembled successfully. According to the curve 'b' (Ip_a = 13.7 μA, Ep_a = 0.227 V, Ip_c = 14.5 μA and Ep_c = 0.160 V), it can be documented that the peak currents of redox peaks are increased rapidly after assembling poly (Gly) with HRP–SiSG on the CPE and this was due to the excellent electron transfer ability of poly (Gly) in between the enzyme and the electrode. The curve 'a' (Ip_a = 15.4 μA, Ep_a = 0.231 V, Ip_c = 15.3 μA and Ep_c = 0.154 V) shows the increase in the redox peak currents on adding MWCNTs to the above combination electrode and this was due to the good electrical conductivity of MWCNTs.

3.3. Electrocatalytic response of DA at HRP–MWCNTs–SiSG/Poly (Gly)/CPE

Fig. 3 demonstrates the cyclic voltammograms obtained for the electrochemical response of 1 mM DA at the bare CPE (curve 'b'), MWCNTs/Poly (Gly)/CPE (curve 'c') and HRP–MWCNTs–SiSG/Poly (Gly)/CPE (curve 'd') in 0.1 M PBS (pH 7.0)/1 M KCl (curve 'a') at a scan rate of 50 mV s^{-1}. At the bare CPE, the oxidation (Ep_a) and reduction (Ep_c) peak potentials occurred at 0.192 V and 0.094 V respectively and corresponding peak potentials difference (ΔE_p) was found to be 98 mV. The anodic and cathodic peak current ratio (Ip_a/Ip_c) was about 1.7, which were the characteristics of quasireversible electrode process. Under the similar conditions, the Ep_a and Ep_c peak potentials occurred at 0.179 V, 0.134 V for MWCNTs/Poly (Gly)/CPE and 0.171 V, 0.123 V for HRP–MWCNTs–SiSG/Poly (Gly)/CPE. The ΔE_p values were found to be 45 mV, 48 mV and Ip_a/Ip_c were 1.1, 1.3 for MWCNTs/Poly (Gly)/CPE and HRP–MWCNTs–SiSG/Poly (Gly)/CPE electrodes respectively, and these represent the characteristics of reversible electrode process. The remarkable enhancement of peak currents provides the clear evidence of the catalytic effect of the biosensor.

The surface concentration of electroactive HRP (Γ) in HRP–SiSG/MWCNTs/Poly (Gly)/CPE was estimated according to Faraday laws as follows [34].

$$\mathrm{Ip} = \frac{n^2F^2A\Gamma\nu}{4RT} \quad (1)$$

where Ip is the reduction peak current, A is the electrode active surface area, ν is the scan rate, n is the number of electrons, R, T and F has their usual meanings. By using the above mentioned equation (1) the value of Γ was calculated as 1.15×10^{-7} mol cm^{-2}. The amount of electroactive HRP was more than 5.00×10^{-11} mol cm^{-2}, which was a saturated concentration of HRP in one layer [35], indicating the formation of multiple layers of HRP on the electrode surface. This indicates the multiple but not the single layer formed on the electrode surface. The MWCNTs–SiSG/Poly (Gly)/CPE immobilization matrix was of more efficient for the HRP immobilization. The surface concentration of electroactive HRP (Γ) with different immobilization matrices was compared with the present immobilization matrix in Table 1.

3.4. Influence of the solution pH

The effect of pH (5.5–8.5) on the electrochemical responses of biosensor towards the determination of DA was studied in 0.1 M PBS/1 M KCl solution. As shown in Fig. 4, the peak currents of DA reached maximum at pH 7.0, and then decrease gradually with increase in pH. Hence for further experimental analysis pH 7.0 was selected. The peak potentials were shifted from 0.22 V to 0.06 V with increasing pH of the solution from 5.5 to 8.5. The potential diagram was constructed by plotting the graph of Ep_a/Ip_a vs. pH of the solution and it was shown as inset of Fig. 4 and the linear regression equation was found to be Ep_a (V) = 0.5274–0.0566 pH (r^2 = 0.9899). The graph has good linearity with a slope of 56 mV/pH, this value was nearly close to the theoretical value (59 mV/pH) of the Nernst equation for equal number of electrons and protons transfer reaction [43].

3.5. Effect of scan rate

The effect of scan rate for DA in 0.1 M PBS (pH 7.0)/1 M KCl was studied at the developed biosensor electrode by CV. The redox peak currents were increased by increasing the scan rate from 50 mV s^{-1}

Table 1
Michaelis–Menten constant and Γ values for HRP in different biosensors.

Biosensor	Γ[a]	K_m^{app}[b]	[Ref.]
HRP/MPA[c]/Au[d]	5×10^{-11} mol cm^{-2}	–	[35]
HRP/DPPA[e]/PGE[f]	1.5×10^{-10} mol cm^{-2}	–	[36]
HRP/nano-Au/ch[g]/GCE[h]	1.2×10^{-9} mol cm^{-2}	1.55 mM	[37]
HRP/nano-Au/Cys[i]/SiSG[j]/Au	–	1.1 mM	[38]
HRP/Colloidal Au/CPE[k]	7.5×10^{-11} mol cm^{-2}	3.69 mM	[39]
HRP/Colloidal Au/SPCE[l]	–	1.3 mM	[40]
HRP/MB[m]/MWCNTs[n]/GCE	3.2×10^{-12} mol cm^{-2}	0.12 mM	[41]
CPE/sol–gel–Fer[o]/HRP/sol-gel	–	0.19 mM	[42]
HRP–MWCNTs–SiSG/Poly (Gly)[p]/CPE	1.15×10^{-7} mol cm^{-2}	0.5 mM (for DA)	Present work

[a] Γ – Electroactive concentration of HRP on the immobilized electrode surface.
[b] K_m^{app} – Apparent Michaelis–Menten constant.
[c] MPA – 3-mercaptopropionic acid.
[d] Au – Gold electrode.
[e] DPPA – Dipalmitoylphosphatidic acid.
[f] PGE – Pyrolytic graphite electrode.
[g] ch – Choline.
[h] GCE – Glassy carbon electrode.
[i] Cys – Cysteine.
[j] SiSG – Silica sol–gel
[k] CPE – Carbon paste electrode.
[l] SPCE – Screen printed carbon electrode.
[m] MB – Methylene blue.
[n] MWCNTs – Multiwalled carbon nanotubes.
[o] Fer – Ferrocene.
[p] Poly (Gly) – Poly (Glycine).

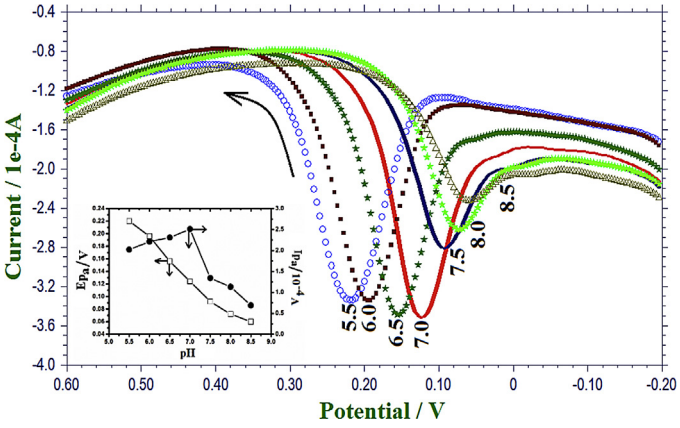

Fig. 4. The differential pulse voltammograms of biosensor with different pH of 0.1 M PBS/1 M KCl containing 1 mM DA. Inset: Relationship of Ep_a/Ip_a vs. pH.

to 130 mV s^{-1} and the same was shown in Fig. 5(A). The graph showed good linearity between the square root of scan rate ($\upsilon^{1/2}$) and redox peak currents with correlation coefficients (r^2) of 0.9931 and 0.9912 for $\upsilon^{1/2}$ vs. Ip_a and $\upsilon^{1/2}$ vs. Ip_c respectively. These results indicate that the electron transfer reactions of biosensor were diffusion controlled process.

In order to support the DA electrochemical reaction mechanism, the variation of the peak potentials as a function of the scan rate was analyzed. The anodic potentials depend linearly on the logarithm of the scan rate as predicted by Eqs. (2) and (3) proposed by Aoki et al. [44].

$$Ep_a = E_o + m[0.78 + \ln\left(\frac{D^{1/2}}{K^o}\right) - 0.5\ln m] + 0.5m\ln\ \upsilon \quad (2)$$

$$m = \frac{RT}{[(1-\alpha)nF]} \quad (3)$$

where 'E_o' is the formal potential of DA, 'D' is the diffusion coefficient, 'K^o' is the heterogeneous standard rate constant, 'α' is the energy transfer coefficient and 'n' is the number of electrons transferred during the heterogeneous reaction. R, F and T are the universal gas constant, Faraday constant and absolute temperature respectively. The formal potential of DA was deduced from the intercept of Ep vs. υ plot. From Eq. (4) [45], it is possible to calculate the value of the energy transfer coefficient (α) from the Fig. 5(C) as 0.368. The 'α' value and the slope obtained from the Fig. 5(B) was substituted in Eq. (3) and from the calculation, the number of electrons involved during DA two step oxidation processes was found to be 0.90 (≈1). From these results it is possible to conclude that

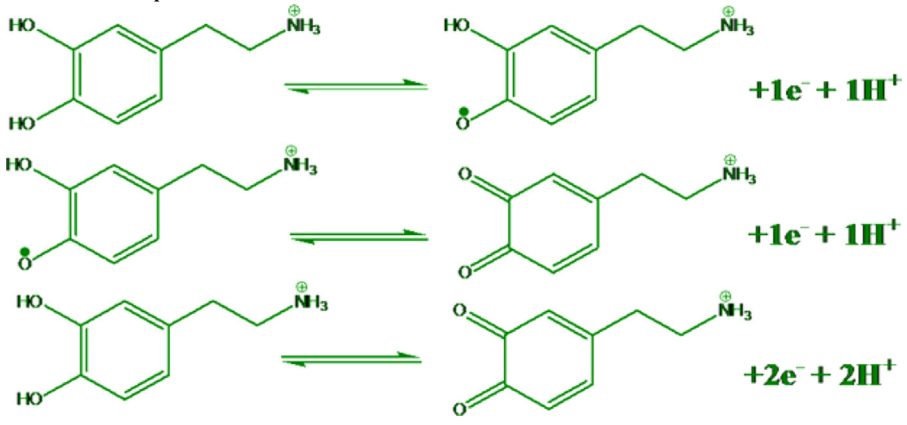

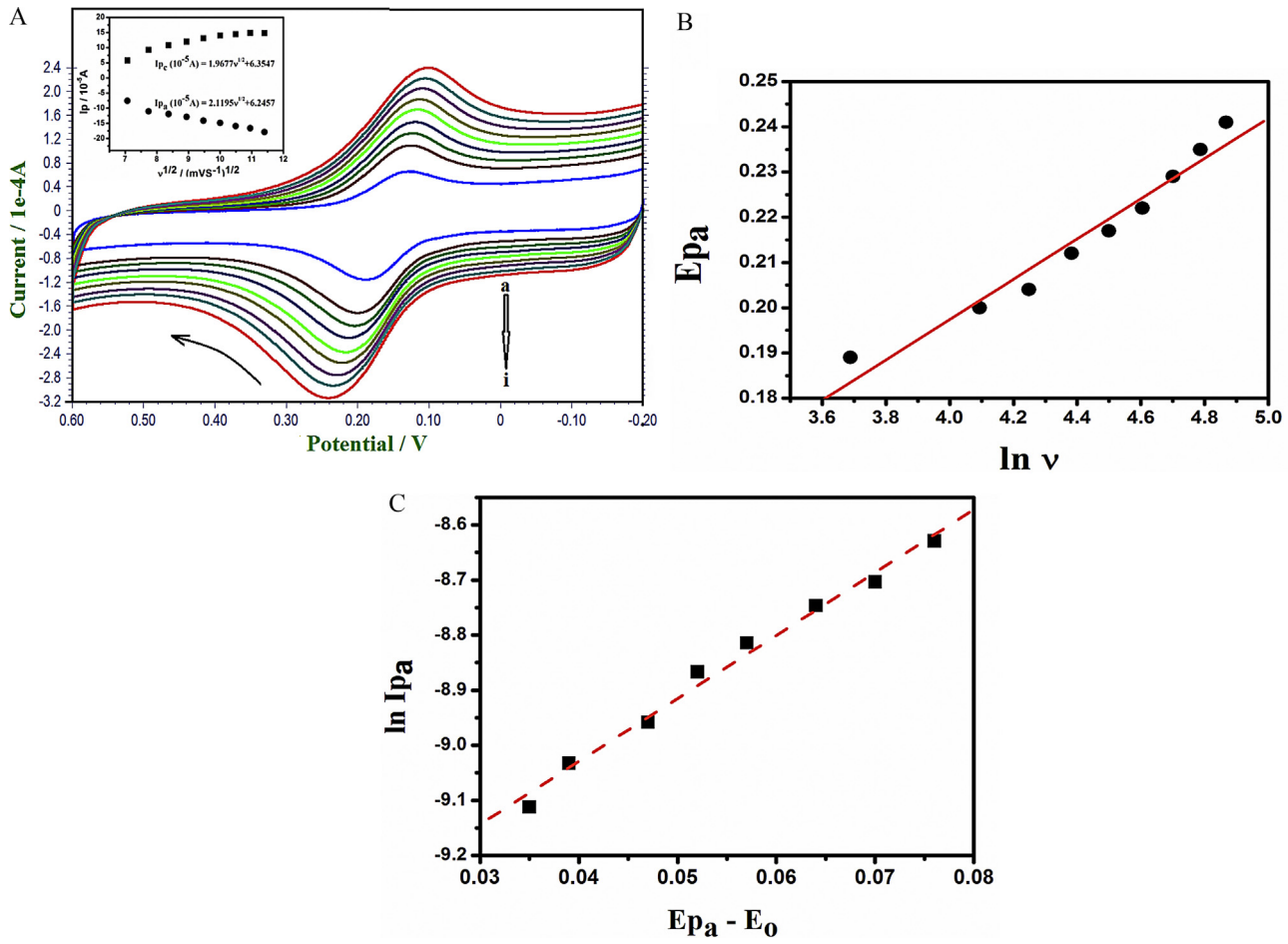

Fig. 5. [A] The cyclic voltammograms of biosensor with different scan rates a→50 mV s^{-1}, b→60 mV s^{-1}, c→70 mV s^{-1}, d→80 mV s^{-1}, e→90 mV s^{-1}, f→100 mV s^{-1}, g→110 mV s^{-1}, h→120 mV s^{-1}, i→130 mV s^{-1} in 0.1 M PBS/1 M KCl containing 1 mM DA. Inset: Relationship between Ip vs. $\nu^{1/2}$. [B] Relation between peak potential (Ep_a) and the scan rate (ln ν). [C] Experimental variation of peak current (ln Ip_a) as a function of the difference $Ep_a - E_o$.

DA oxidation occurs through monoelectronic steps as indicated in (R1 and R2).

$$i_p = 0.227FAC_o^* K^o \exp[-\alpha f(E_p - E^o)] \quad (4)$$

where A is the electrode surface area, C_o^* is the DA concentration and $f = F/RT$.

To determination of the values of K^o from experimental ΔE_p values, Eq. (5) was a valid approximation of such curves for $\Delta E_p > 10$ mV and the results were reported in Table 2.

$$\Delta E_p = 201.39 \log\left(\frac{\upsilon}{K^o}\right) - 301.78 \quad (5)$$

Table 2
Electrochemical parameters of DA at different scan rates.

ν/mV s^{-1}	ΔE_p/mV	K^o/s^{-1}
60	75	0.809
70	81	0.881
80	93	0.877
90	101	0.901
100	109	0.912
110	120	0.885
120	129	0.871
130	140	0.832

3.6. Electrocatalytic oxidation of DA at HRP–MWCNTs–SiSG/Poly (Gly)/CPE (biosensor)

Fig. 6 shows the typical DPV response of the biosensor for successive additions of DA under optimized conditions. It was clear that a rapid and sensitive response of DA was achieved due to the

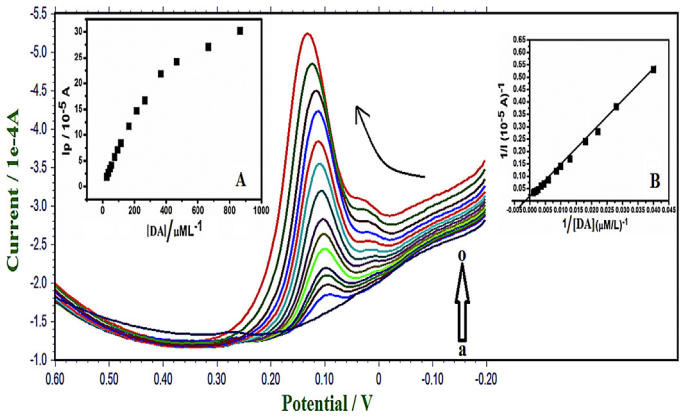

Fig. 6. Typical differential pulse voltammograms of (a) 0 μM, (b) 15 μM, (c) 30 μM, (d) 45 μM, (e) 55 μM, (f) 75 μM, (g) 95 μM, (h) 115 μM, (i) 165 μM, (j) 215 μM, (k) 265 μM, (l) 365 μM, (m) 465 μM, (n) 665 μM, (o) 865 μM for DA in 0.1 M PBS/1 M KCl. Inset: [A] Calibration plot of Ip vs. [DA]. [B] Lineweaver–Burk plot for DA.

presence of matrix immobilized on the electrode surface, which facilitated the efficient electron transfer rate. The inset [A] of Fig. 6 shows the calibration curve between the biosensor response and the DA concentration. Excellent linear relationship was obtained in the concentration range of 15–165 μM with the linear regression equation of Ip (10^{-5} A) = −0.0075 + 0.076C (μM), (r^2 = 0.9993). The LOD and LOQ of this biosensor were estimated as 6×10^{-7} M and 2×10^{-6} M respectively. The LOD and LOQ values were calculated by using the following equations [46,47].

$$\mathrm{LOD} = \frac{3S_b}{S} \quad (6)$$

$$\mathrm{LOQ} = \frac{10S_b}{S} \quad (7)$$

where S_b is the standard deviation of mean values for 10 differential–pulse voltammograms of blank solution, S is the slope of the working curve. The apparent Michaelis–Menten constant (K_m^{app}), gives the information of enzyme substrate kinetics and also the enzymatic affinity and can be calculated from the electrochemical version of the Linewever–Burk equation [48].

$$\frac{1}{i_s} = \frac{1}{i_{max}} + \frac{K_m^{app}}{i_{max}C} \quad (8)$$

where 'i_s' is the steady current after the addition of substrate and 'i_{max}' is the maximum current measured under saturated substrate condition. The K_m^{app} was determined from the slope and intercept for the calibration plot of reciprocals of current vs. DA concentration and was illustrated in the inset [B] of Fig. 6. The immobilized enzyme showed K_m^{app} and i_{max} values of 0.5 mM and 0.4 mA respectively. The K_m^{app} was smaller than reported result for HRP immobilized in sol–gel derived ceramic–carbon nanotube nanocomposite film (23.85 mM) [49]. The smaller K_m^{app} indicates the immobilized HRP posse's high catalytic affinity towards the oxidation of DA.

3.7. Investigation of electrochemical behavior of various film modified electrodes using EIS studies

The Electrochemical impedance spectroscopy (EIS) is an effective technique for studying the interfacial properties of various surface modified electrodes. The electron transfer resistance (R_{et}) controls the interfacial electron transfer rate of the modified electrodes. Its values were varied when different types of modifier substances are adsorbed on the surface of the electrode [50]. The EIS measurements were carried out in a solution of 5 mM K_3 [Fe (CN_6)]/K_4 [Fe (CN_6)] and 1 M KCl at a initial potential of 0.0653 V, the alternating voltage of 5 mV and the frequency range between 1 Hz and 1×10^5 Hz.

Fig. 7 presents the impedance spectrum of different modified electrodes. The R_{et} values were obtained by fitting the equivalent circuit (Inset). It was observed that the bare CPE (a) with (R_{et} = 28.3 Ω), after being immobilized with enzyme solution on the surface of CPE i.e. HRP–SiSG/CPE (b) (R_{et} = 36.5 Ω) exhibits more resistance than CPE, due to the blocking of active sites of electrode. To the above mentioned electrode MWCNTs was added i.e. HRP–MWCNTs–SiSG/CPE (c) and found (R_{et} = 17.9 Ω). We observed the decrease in resistance values and this was due to the good conductivity of MWCNTs. The polymerized CPE i.e. poly (Gly)/CPE (e) (R_{et} = 10.5 Ω) showed least resistance of the all electrodes because of excellent conductivity between the K_3 [Fe (CN_6)]/K_4 [Fe (CN_6)] and surface of the electrode. To the polymerized electrode HRP was added i.e. HRP–SiSG/poly (Gly)/CPE (d) and found (R_{et} = 14.6 Ω) later MWCNTs was added to the above electrode i.e. HRP–MWCNTs–SiSG/Poly (Gly)/CPE (f) and found (R_{et} = 11.3 Ω). From the results, we concluded that for every addition of enzyme solution onto the surface of different composite electrodes, there

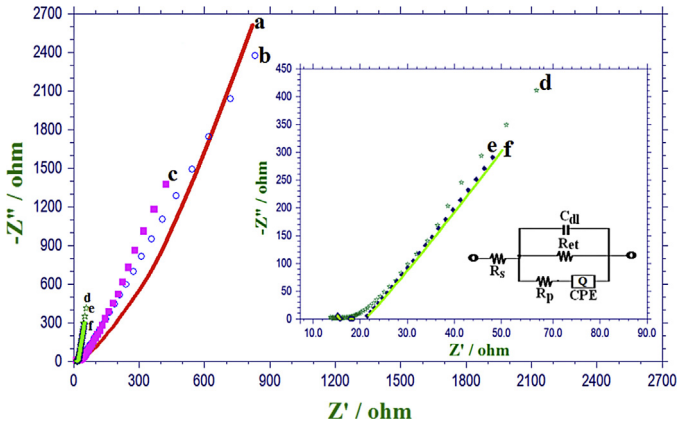

Fig. 7. EIS of (a) bare CPE (b) HRP–SiSG/CPE (c) HRP–MWCNTs–SiSG/CPE (d) HRP–SiSG/poly (Gly)/CPE (e) poly (Gly)/CPE (f) HRP–MWCNTs–SiSG/Poly (Gly)/CPE recorded in 1 M KCl containing 5 mM K_3[Fe(CN_6)]/K_4[Fe(CN_6)], amplitude: 5 mV, frequency: 1 Hz to 100 kHz.

was a rise in R_{et} values. Therefore, we confirmed that the HRP was successfully immobilized on the electrode surface.

3.8. Interference study at the biosensor

The selectivity of the biosensor was investigated by detecting 0.2 mM of DA in the presence of several possible coexisting interferences such as uric acid, ascorbic acid, serotonin, tyrosine, aspartic acid, serine and cysteine. The results are reported in Table 3. The current ratio were calculated by measuring the current of the biosensor in 0.1 M PBS/1 M KCl containing 0.2 mM of DA and 1 mM interfering substance (I_1) and comparing it with the current of biosensor in 0.1 M PBS/1 M KCl containing only 0.2 mM of DA (I_2). The degree of interference from the substances can be judged from the values of current ratio. From the results, we concluded that the developed biosensor exhibits an excellent selectivity towards the determination of DA, since there was no significant change in the current ratio with the interferences.

3.9. Stability and reproducibility of the biosensor

The stability of the developed biosensor was studied by performing 50 multiple successive cycles in the potential range from −0.2 V to 0.6 V at a scan rate of 50 mV s^{-1} in 0.1 M PBS (pH 7.0)/1 M KCl containing 1 mM of DA, it was observed that after 50 cycles there was no much disturbance in the peak potentials of the system, whereas the peak currents of the system reduced to 89% in comparison with the initial signal. This indicates that immobilized enzyme matrix was stably fixed onto the electrode surface. In terms of repeatability a relative standard deviation (RSD) of 3.5% was estimated at 1 mM of DA. The reproducibility of the biosensor was investigated by constructing four enzyme electrodes and these were tested in 1 mM of DA and found an RSD of 4.3%. The biosensor

Table 3
Effect of possible interferants on the biosensor.

Interferants	Current ratio (I_1/I_2)	%RSD[a]
Uric acid	0.88	1.92
Ascorbic acid	0.96	1.65
Serotonin	0.98	1.47
Tyrosine	0.93	1.75
Aspartic acid	1.01	1.21
Serine	0.94	1.95
Cysteine	1.13	2.03

[a] Four number of assay.

Table 4A
Detection of DA in injection samples.

Sample	Content (mg/ml)	Found[a] (mg/ml)	%RSD	Recovery (%)	Bias
1	4.0	3.95	2.5	98.7	−1.25
2	4.0	3.91	2.9	98	−2.25
3	4.0	4.02	2.1	100.5	+0.5
4	4.0	3.97	2.3	99	−0.75

[a] Average for four determinations.

Table 4B
Comparison of different electrochemical techniques for the determination of DA.

Electrode	LOD/ML^{-1}	Technique	Ref.
Metallothioneins self-assembled gold electrode	6×10^{-6}	CV	[51]
Ionic liquid modified carbon paste electrode	7×10^{-7}	CV	[52]
Poly (caffeic acid)/GCE	2×10^{-7}	CV	[53]
α-CD/CNT/PGE	1×10^{-6}	DPV	[54]
Poly (p-toluene sulfonic acid) modified glassy carbon electrode	6×10^{-7}	DPV	[55]
Poly(solo chrome dark blue) modified carbon paste electrode	8×10^{-7}	DPV	[56]
HRP–MWCNTs–SiSG/Poly (Gly)/CPE	6×10^{-7}	DPV	Present work

electrode showed a comparable stable activity when stored in 0.1 M PBS (pH 7.0) for up to 2 weeks in the refrigerator at 4 °C.

3.10. Analytical application

The biosensor was applied for the determination of dopamine hydrochloride injection. The DA injection sample purchased from sterile specialties India Pvt. Ltd., with a specified content of DA 40 mg/ml. The samples were examined after suitable dilution with 0.1 mM PBS. The results were reported in Table 4A. The recovery and RSD were acceptable and showed that the proposed method could be efficiently employed for the determination of DA in injections. Table 4B shows the results obtained at various modified electrodes towards the determination of DA and comparison with the present method.

4. Conclusions

In the present work, we have developed a novel strategy based on the modification of CPE with poly (Gly) and MWCNTs, which facilitates the immobilization of HRP–SiSG and also the electron transfer rate between the enzyme and the surface of the electrode. The biosensor exhibited a remarkable good analytical performance in terms of sensitivity, stability, selectivity, ease of fabrication, low cost and fast response. The proposed biosensor was able to determine DA in the presence of number of interferences and in DA injection samples. We believed that, this approach can be readily applied to the development of reagentless biosensor towards the determination of DA and other neurotransmitters.

Acknowledgment

The authors are gratefully acknowledging the financial support from University Grants Commission (UGC), New Delhi, India, in the form of research project no.F.39-709/2010.

References

[1] Avendano SC, Angeles GA, Silva MTR, Pina GR, Romo MR, Pardave MP. On the electrochemistry of dopamine in aqueous solution. Part I: The role of [SDS] on the voltammetric behavior of dopamine on a carbon paste electrode. J Electroanal Chem 2007;609:17–26.
[2] Yao H, Sun Y, Lin X, Tang Y, Huang L. Electrochemical characterization of poly (eriochrome black T) modified glassy carbon electrode and its application to simultaneous determination of dopamine, ascorbic acid and uric acid. Electrochim Acta 2007;52:6165–71.
[3] Li J, Lu J. Flow-injection/chemiluminescene assays of catecholamines. Chin J Anal Chem 1997;25:314–6.
[4] Nohta H, Yukizawa T, Yoshimura M, Ishida J, Yamaguchi M. Aromatic glycinonitriles and methylamines as pre-column fluorescence derivatization reagents for catecholamines. Anal Chim Acta 1997;344:233–40.
[5] Wu Y, Fan R, Di J. Electrochemical study of electron transfer between dopamine and ferrocene at liquid/liquid interface. Chin J Anal Chem 1996;24:873–5.
[6] Zhu R, Kok WT. Determination of catecholamines and related compounds by capillary electrophoresis with postcolumn terbium complexation and sensitized luminescence detection. Anal Chem 1997;69:4010–6.
[7] Sarre S, Michotte Y, Herregodts P, Deleu D, Klippel ND, Ebinger G. High-performance liquid chromatography with electrochemical detection for the determination of levodopa, catecholamiine and their metabolites in rat brain dialysates. J Chromatogr 1992;575:207–12.
[8] Guan CL, Ouyang J, Li QL, Liu BH, Baeyens WRG. Simultaneous determination of catecholamines by ion chromatography with direct conductivity detection. Talanta 2000;50:1197–203.
[9] Xiao LP, Chen J, Cha CS. Elimination of the interference of ascorbic acid in the amperometric detection of biomolecules in body fluid samples and the simple detection of uric acid in human serum and urine by using the powder microelectrode technique. J Eletroanal Chem 2000;495:27–35.
[10] Rekha, Kumara Swamy BE, Deepa R, Krishna V, Gilbert O, Chandra U, et al. Electrochemical investigations of dopamine at chemically modified alcian blue carbon paste electrode: a cyclic voltammetric study. Int J Electrochem Sci 2009;4:832–45.
[11] Valentini F, Amine A, Orlanducci S, Terranova ML, Palleschi G. Carbon nanotube purification: preparation and characterization of carbon nanotube paste electrodes. Anal Chem 2003;75:5413–21.
[12] Liu J, Chau A, Rahmat W, Paddon-Row MN, Gooding JJ. Achieving direct electrical connection to glucose oxidase using aligned single walled carbon nanotube arrays. Electroanalysis 2005;17:38–46.
[13] Joseph S, Rusling JF, Lvov YM, Friedberg J, Fuhr YM. An amperometric biosensor with human CYP3A4 as a novel drug screening tool. Biochem Pharmacol 2003;65:1817–26.
[14] Kotz E, Willner I. Biomolecule-functionalized carbon nanotubes: applications in nanobioelectronics. Chemphys Chem 2004;5:1084–94.
[15] Gong K, Yan Y, Zhang M, Su L, Xiong S, Mao L. Biomolecule-functionalized carbon nanotubes: applications in nanobioelectronics. Anal Sci 2005;21:1383–93.
[16] Ajayan PM. Nanotubes from carbon. Chem Rev 1999;99:1787–90.
[17] Liu BH, Liu ZJ, Chen DD, Kong JL, Deng JQ. An amperometric biosensor based on the coimmobilization of horseradish peroxidase and methylene blue on a beta-type zeolite modified electrode. Fresenius J Anal Chem 2000;367:539–44.
[18] Cao DF, He PL, Hu NF. Electrochemical biosensors utilising electron transfer in heme proteins immobilised on Fe_3O_4 nanoparticles. Analyst 2003;128:1268–74.
[19] Utpal B, Pragya S, Krishnamoorthy K, Pradip N. Photoreactive cellulose membrane – a novel matrix for covalent immobilization of biomolecules. J Biotechnol 2006;126:220–9.
[20] Saroj K, Pradip N. Sunlight-induced covalent immobilization of proteins. Talanta 2007;71:1438–40.
[21] Qu S, Huang F, Chen G, Yu SN, Kong JL. Magnetic assembled electrochemical platform using Fe_2O_3 filled carbon nanotubes and enzyme. Electrochem Commun 2007;9:2812–6.
[22] Wang JW, Gu M, Di JW, Gao YS, Wu Y, Tu YF. A carbon nanotube/silica sol–gel architecture for immobilization of horseradish peroxidase for electrochemical biosensor. Bioprocess Biosyst Eng 2007;30:289–96.
[23] Morrin A, Wilbeer F, Ngamma O, Moulton SE, Killard AJ, Wallace GG, et al. Novel biosensor fabrication methodology based on processable conducting polyaniline nanoparticles. Electrochem Commun 2005;7:317–22.
[24] Shao Y, Jin YD, Wang JL, Wang L, Zohao F, Dong SJ. Conducting polymer polypyrrole supported bilayer lipid membranes. Biosens Bioelectron 2005;20:1373.

[25] Jin W, Brennan JD. Properties and applications of proteins encapsulated within sol–gel derived materials. Anal Chim Acta 2002;461:1–6.
[26] Aurobind SV, Amirthalingam KP, Gomathi H. Sol-gel based surface modification of electrodes for electro analysis. Adv Colloid Interface Sci 2006;121:1–7.
[27] Wang G, Xu JJ, Chen HY, Lu ZH. Amperometric hydrogen peroxide biosensor with sol–gel/chitosan network-like film as immobilization matrix. Biosens Bioelectron 2003;18:335–43.
[28] Rosatto SS, Sotomayor PT, Kubota LT, Gushikem Y. SiO_2/Nb_2O_5 sol–gel as a support for HRP immobilization in biosensor preparation for phenol detection. Electrochim Acta 2002;47:4451–8.
[29] Chen X, Wang BQ, Dong ST. Amperometric biosensor for hydrogen peroxide based on sol-gel/hydrogel composite thin film. Electroanalysis 2001;13:1149–52.
[30] Lei CX, Hu SQ, Gao N, Sehn GL, Yu RQ. An amperometric hydrogen peroxide biosensor based on immobilizing horseradish peroxidase to a nano-Au monolayer supported by sol–gel derived carbon ceramic electrode. Bioelectrochemistry 2004;65:33–9.
[31] Raghu P, Kumara Swamy BE, Madhusudana Reddy T, Chandrashekar BN, Reddaiah K. Sol–gel immobilized biosensor for the detection of organophosphorous pesticides: a voltammetric method. Bioelectrochemistry 2012;83:19–24.
[32] Raghu P, Madhusudana Reddy T, Kumara Swamy BE, Chandrashekar BN, Reddaiah K, Sreedhar M. Development of AChE biosensor for the determination of methyl parathion and monocrotophos in water and fruit samples: a cyclic voltammetric study. J Electroanal Chem 2012;665:76–82.
[33] Anitha K, Venkata Mohan S, Jayarama Reddy S. Development of acetylcholinesterase silica sol–gel immobilized biosensor—an application towards oxydemeton methyl detection. Biosens Bioelectron 2004;20:848–56.
[34] Laviron E. The use of linear potential sweep voltammetry and of a.c. voltammetry for the study of the surface electrochemical reaction of strongly adsorbed systems and of redox modified electrodes. J Electroanal Chem 1979;100:263–70.
[35] Li J, Dong S. The electrochemical study of oxidation-reduction properties of horseradish peroxidase. J Electroanal Chem 1997;431:19–22.
[36] Liu X, Huang Y, Shang L, Wang X, Xiao H, Li G. Electron transfer reactivity and the catalytic activity of horseradish peroxidase incorporated in dipalmitoylphosphatidic acid films. Bioelectrochemistry 2006;68:98–104.
[37] Zheng Y, Qin LX. Modified electrode based on immobilizing horseradish peroxidase on nano-gold with choline covalently modified glassy carbon electrode as a base. Chin J Anal Chem 2008;36:604–8.
[38] Di J, Shen C, Peng S, Tu X, Li S. A one-step method to construct a third-generation biosensor based on horseradish peroxidase and gold nanoparticles embedded in silica sol–gel network on gold modified electrode. Anal Chim Acta 2005;553:196–200.
[39] Liu S, Ju H. Renewable reagentless hydrogen peroxide sensor based on direct electron transfer of horseradish peroxidase immobilized on colloidal gold-modified electrode. Anal Biochem 2002;307:110–6.
[40] Xu X, Liu S, Ju H. A novel hydrogen peroxide sensor via the direct electrochemistry of horseradish peroxidase immobilized on colloidal gold modified screen-printed electrode. Sensors 2003;3:350–60.
[41] Xu JZ, Zhu JJ, Wu Q, Hu Z, Chen HY. An amperometric biosensor based on the coimmobilization of horseradish peroxidase and methylene blue on a carbon nanotubes modified electrode. Electroanalysis 2003;15:219–24.
[42] Chut SL, Li J, Tan SN. Long-term monitoring of polycyclic aromatic hydrocarbons in Mussels (*Mytilus edulis*) following the *Braer* oil spill. Analyst 1997;122:1431–5.
[43] Jones BD, Ingle Jr JD. Evaluation of immobilized redox indicators as reversible, in situ redox sensors for determining Fe(III)-reducing conditions in environmental samples. Talanta 2001;55:699–714.
[44] Aoki K, Akimoto K, Tokuda K, Matsuda H, Osteryoung J. Linear sweep voltammetry at very small stationary disc electrodes. J Electroanal Chem 1984;171:219–20.
[45] Bard AJ, Faulkner LR. Electrochemical methods: fundamentals and applications. New York: Wiley; 2000.
[46] Madhusudana Reddy T, Reddy SJ. Differential pulse adsorptive stripping voltammetric determination of nifedipine and nimodipine in pharmaceutical formulations, urine, and serum samples by using a clay-modified carbon-paste electrode. Anal Lett 2004;37:2079–88.
[47] Madhusudana Reddy T, Sreedhar M, Reddy SJ. Voltammetric behavior of cefixime and cefpodoxime proxetil and determination in pharmaceutical formulations and urine. J Pharm Biomed Anal 2003;31:811–8.
[48] Kamin RA, Wilson GS. Rotating ring-disk enzyme electrode for biocatalysis kinetic studies and characterization of the immobilized enzyme layer. Anal Chem 1980;52:1198–205.
[49] Chen HJ, Dong SJ. Direct electrochemistry and electrocatalysis of horseradish peroxidase immobilized in sol–gel-derived ceramic–carbon nanotube nanocomposite film. Biosens Bioelectron 2007;22:1811.
[50] Liu YJ, Yin F, Long YM, Zhang ZH, Yao SZ. Study of the immobilization of alcohol dehydrogenase on Au-colloid modified gold electrode by piezoelectric quartz crystal sensor, cyclic voltammetry, and electrochemical impedance techniques. J Colloid Interface Sci 2003;258:75–81.
[51] Wang Q, Li N, Wnag W. Electrocatalytc response of dopamine at a metallothioneins self-assembled gold electrode. Anal Sci 2002;18:635–9.
[52] Sun W, Yang M, Jiao K. Electrocatalytic oxidation of dopamine at an ionic liquid modified carbon paste electrode and its analytical application. Anal Bioanal Chem 2007;389:1283–91.
[53] Li NB, Ren W, Luo HQ. Caffeic acid-modified glassy carbon electrode for the simultaneous determination of epinephrine and dopamine. Electroanalysis 2007;19:1496–502.
[54] Wang GY, Liu XJ, Luo GA, Wang ZH. α-Cyclodextrin incorporated carbon nanotube-coated electrode for the simultaneous determination of dopamine and epinephrine. Chin J Chem 2005;23:297–302.
[55] Huang PF, Wang L, Bai JY, Wang HJ, Zhao YQ, Fan SD. Simultaneous electrochemical detection of dopamine and ascorbic acid at a poly(*p*-toluene sulfonic acid) modified electrode. Microchim Acta 2007;157:41–7.
[56] Reddaiah K, Reddy MM, Raghu P, Reddy TM. An electrochemical sensor based on poly (solochrome dark blue) film coated electrode for the determination of dopamine and simultaneous separation in the presence of uric acid and ascorbic acid: a voltammetric method. Colloids Surf B 2013;106:145–50.